QUANTUM DECOHERENCE FOR HOLOGRAPHIC DUAL OR TOPOLOGICAL ORDERED SYSTEMS

Feng-Li Lin (National Taiwan Normal U) for YQIP 2014@YITP

Based on works 1309.5855 & 1406.6249 with
Sung-Po Chao(NCTS),
Chung-Hsien Chou(NCKU),
Shih-Hao Ho(NCTS),
Wei Li(AEI),
Bo Ning(NTNU)

Quantum decoherence

A. Quantum decoherence can be understood as the leakage of quantum information of an open system. (Joos, Zeh, Zurek)
B. It is a generic phenomenon and explains the emergence of our classical world. E.g.,

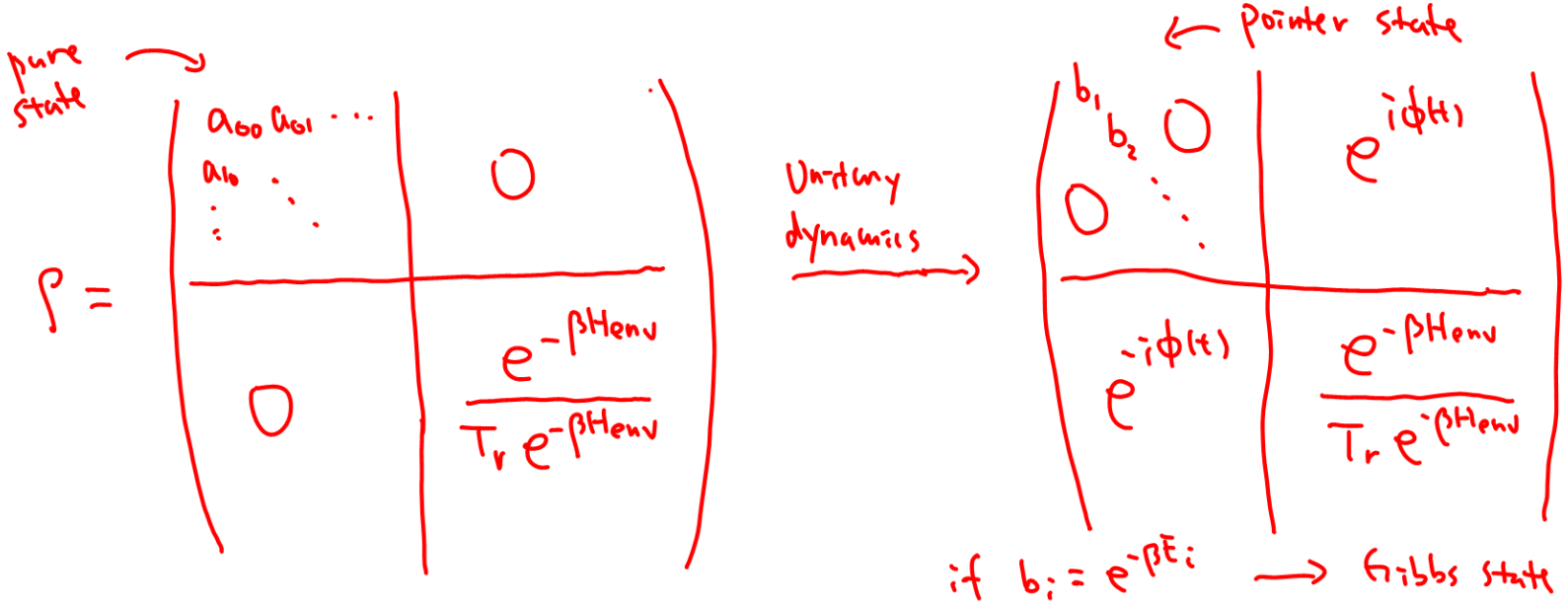

Motivation

A. Quantum deocherence of qubit is an obstacle to realize the realistic quantum computations.
B. The goal of our study is to find the possible candidates for the robust open systems against quantum decoherence.
C. There are many possible ways to achieve the goal, we focus on two effects: The strong interacting environment or the strong correlated open system.

1. The 1st is possible to form localized bound states to cut the information flow.
2. The 2nd is known to be possibly dissipationless.

Our approaches

1) For strongly interacting environment, we consider the cases for which the real time dynamics can be computed by using the gravity duals in the context of AdS/CFT correspondence.
2) For strongly correlated cases, we consider a special system made of topological modes in the context of topological insulator/superconductor.

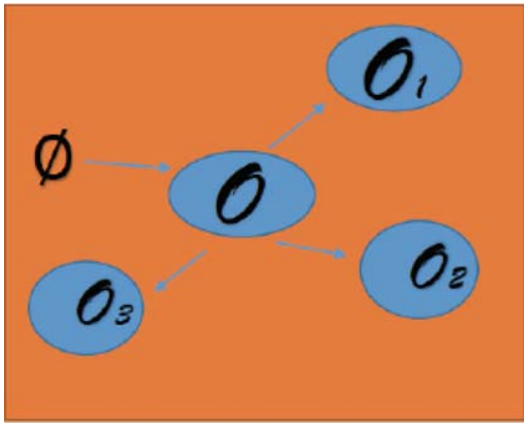

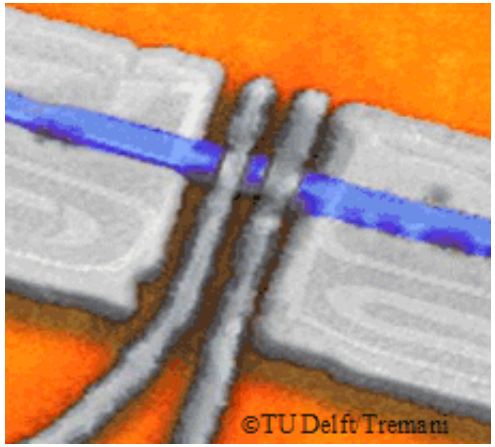

I. Decoherence in holographic environments

Effective probe dynamics

1. Consider a the bilinear coupling between probe ϕ and an operator $\mathcal{O}[\chi]$ of the CFT:

$$g\phi\mathcal{O}[\chi]$$

2. The backaction of $\mathcal{O}[\chi]$ to ϕ causes information loss of ϕ , ie, the reduced dynamics is non-unitary and possibly non-Markovian, ie, information backflow.

3. Formally, this can be obtained by integrating out the environment to get the backaction (influence functional). Then, the probe dynamics is dictated by this effective theory and can be used to study quantum decoherence.

Influence functional

1. Treat the probe as the source to the CFT operator $\mathcal{O}[\chi]$, then the influence functional is the generating function of the correlators of $\mathcal{O}[\chi]$, ie, $\mathcal{F}[\phi] = \langle e^{ig\phi\mathcal{O}[\chi]} \rangle_\chi$

2. The effective dynamics of the probe is encoded in the effective action: $I_{kinetic}[\phi] + \ln \mathcal{F}[\phi]$.

3. In AdS/CFT, the generating function can be computed by evaluating the dual bulk action via GKP/W, i.e.,

$$\langle e^{ig\phi\mathcal{O}[\chi]} \rangle_\chi = e^{iI_{bulk}^{(on-shell)}[\Phi|_\phi]}$$

AdS/CFT correspondence (Maldacena,1997)

1. The holographic principle is manifested in the AdS/CFT correspondence:
2. Effective theory of strongly coupled CFT =1D higher anti-de Sitter gravity.
3. The radial direction is the RG scale of CFT.

$$\langle e^{ig\phi\mathcal{O}[\chi]}\rangle_{\chi} = e^{iI_{bulk}^{(on-shell)}[\Phi[\phi]}$$

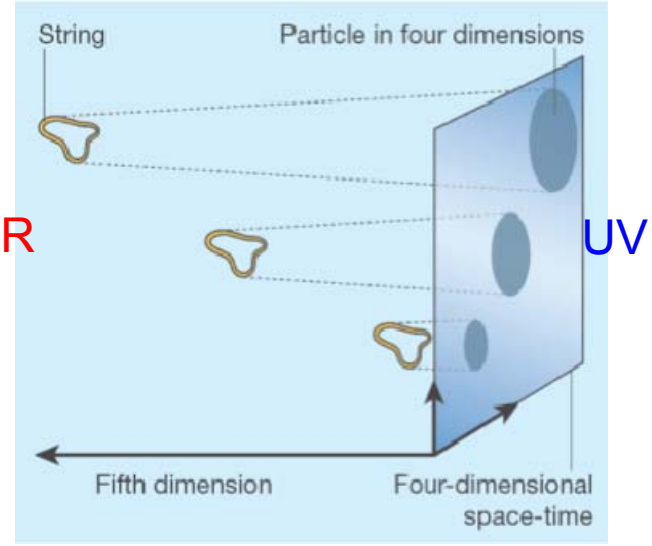

Real time dynamics

1. As we like to consider decoherence, we need to obtain the dynamics of redued density matrix for the probe, i.e.,

$$\rho_{sys}(t) = Tr_{env}\{e^{-iH_{total}t}\rho_{sys}(0)\otimes\rho_{env}(0)e^{iH_{total}t}\}$$

$$H_{total} = H_{sys}[\phi] + H_{env}[\chi] + g\int \phi\mathcal{O}[\chi]$$

2. We should generalize the previous (holographic) forumulation to the real-time contour: $\Sigma = \frac{1}{2}(\phi_+ - \phi_-), \qquad \Delta = \phi_+ - \phi_-$

$$-i\ln\mathcal{F} = -g^2\int_{t_i}^{t_f} d\tau \int_{t_i}^{t_f} d\tau' \int d^dx\, d^dx' \,[\Delta(x)G_R(x-x')\Sigma(x') - \frac{i}{2}\Delta(x)G_{sym}(x-x')\Delta(x')]$$

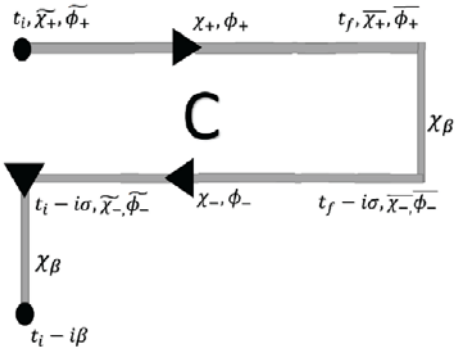

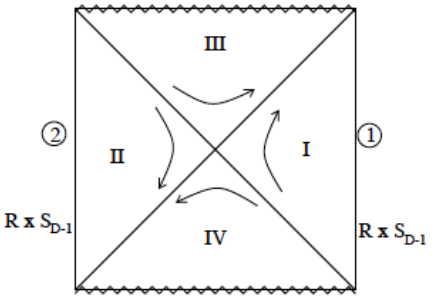

c.f. Herzog & Son 02

Dynamics of open system

1. From the effective action, derive Langevin eq. i.e., $G_R(t)$ is the dissipation kernel, $G_{sym}(t)$ is the fluctuation kernel.

$$\ddot{\Sigma} + m^2\Sigma + g^2 \int^{\tau} d\tau' G_R(\tau - \tau')\Sigma(\tau') = \xi(\tau)\,, \qquad \langle \xi(\tau)\xi(\tau')\rangle = g^2\, G_{sym}(\tau - \tau')$$

2. For thermal bath environment, the KMS condition yields fluctuation-dissipation theorem:

$$G_{sym}(\omega) = -[1 + 2n(\omega)]\mathrm{Im}G_R(\omega)$$

3. On the other hand, one can derive the kernel for the reduced density matrix, i.e., (c.f. Hu et al 92, Caldeira et al, 83)

$$J\left[\bar{\phi}_+, \bar{\phi}_-; t_f | \tilde{\phi}_+, \tilde{\phi}_-; t_i\right] \equiv \int_{\tilde{\phi}_+}^{\bar{\phi}_+} \mathcal{D}\phi_+ \int_{\tilde{\phi}_-}^{\bar{\phi}_-} \mathcal{D}\phi_-\; e^{i\int_{t_i}^{t_f} dt\, (\mathcal{L}_{\rm sys}[\phi_+] - \mathcal{L}_{\rm sys}[\phi_-])} \mathcal{F}[\phi_+, \phi_-]$$

$$\langle \bar{\phi}_+ | \hat{\rho}_{\rm sys}(t_f) | \bar{\phi}_- \rangle = \int d\tilde{\phi}_+ d\tilde{\phi}_- J\left[\bar{\phi}_+, \bar{\phi}_-; t_f | \tilde{\phi}_+, \tilde{\phi}_-; t_i\right] \langle \tilde{\phi}_+ | \hat{\rho}_{\rm sys}(t_i) | \tilde{\phi}_- \rangle$$

Holographic Dissipation Kernel

We consider two holographic cases:

1) A bulk string probe in BTZ black hole = dual of a Brownian particle. The holographic dissipation kernel is Ohmic type: (c.f. Son et al 09, de Boer et al 09)

$$G_R(\omega) = -iN_{st}^2\left(\omega^3 + 4\pi^2 T^2\omega\right)\frac{\Gamma_w^2}{\Gamma_w^2+\omega^2}$$

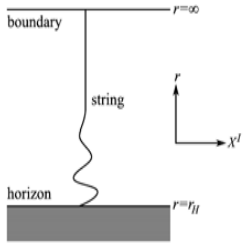

2) A bulk scalar zero mode probe in AdS5 = dual of a scalar zero mode coupled to an operator of conformal dimension Δ in CFT vacuum. The holographic dissipation kernel is quasi-Ohmic type:

$$G_R(\omega) \propto (\omega^2)^{2\Delta-2}[\ln\omega^2 - i\pi\,\mathrm{sgn}(\omega)] \qquad \text{for} \quad \Delta \geq 2$$

Characterizing decoherence

1. One can prepare the two Gaussian wavepackets to mimic the cat state, and then evaluate the Wigner function of the evolving reduced density matrix. Its positivity implies a classical state. (c.f. Zurek, 91)

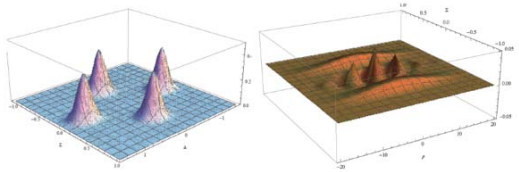

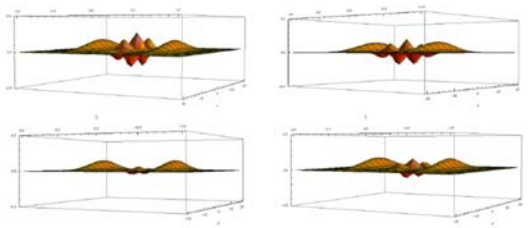

2. Or characterized by the scaling behaviors of the purity, ie, $\mathcal{P} := Tr\rho^2(t), \qquad S_2 := -\ln \mathcal{P}$
3. Concurrence: nonzero for entangled probe states.

The results

1. We plot the negative part of the Wigner function and the 2nd order Renyi entropy for both cases:

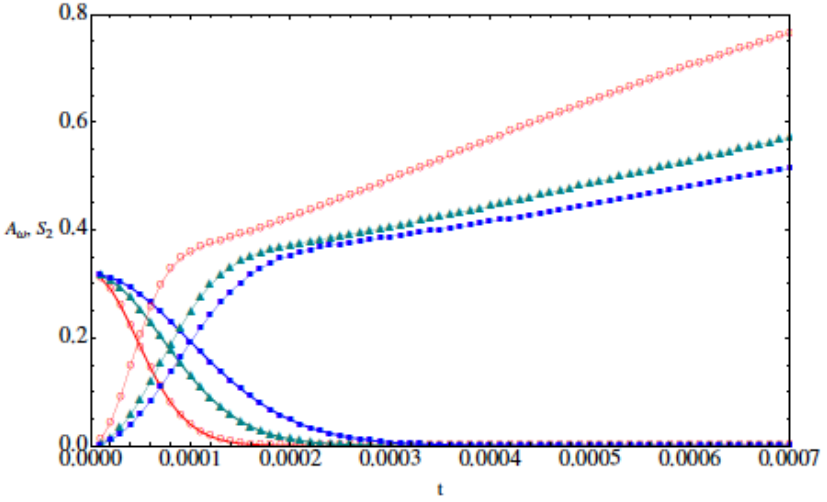

Case 1:
T=50(red), 30(green) and 0.1(blue)

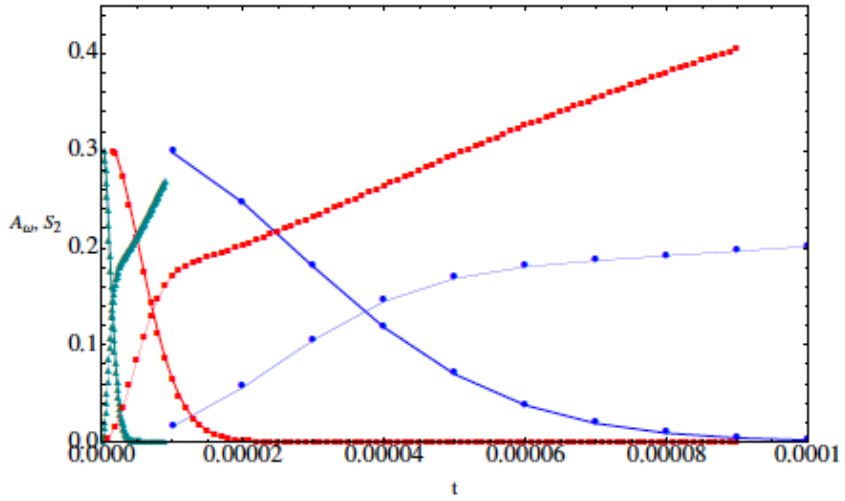

Case 2:
Δ=4.5(green), 4(red) and 3.5(blue)

Summary

1. The decoherence time scale by vanishing of negative part of Wigner function is $\mathcal{O}(1/T)$ for case 1 but $\mathcal{O}(e^{-\Delta})$ for case 2.
2. The Renyi entropy shows a sharp change around the decoherence time scale, it takes much longer time for the probe to be thermalized completely, ie, $S_2 \longrightarrow \infty$
3. The Renyi entropy shows similar scaling behaviors (Right) as for the local holographic quantum quench (Left):

$$S_L(t) \sim \begin{cases} t^2, & t \approx 0\,; \\ t, & t < L\,; \\ \text{const. or} \quad \ln t, & t > L\,. \end{cases}$$

c.f. Liu et al 03

$$S_2(t) \sim \begin{cases} C_0\, t^2\,, & t \approx 0\,; \\ C_{b.c.}\, t\,, & t < t_D\,; \\ C_{a.c.} \ln t\,, & \mathcal{O}(10)\, t_D > t > t_D\,; \\ C_1\, t\,, & t >> t_D\,. \end{cases} \qquad C_{b.c.} > C_1$$

Some discussions

1. Our dissipation kernel is not very different from usual Ohmic type though the environment is strongly interacting.
2. We are considering the holographic environment with more non-conventional holographic dissipation kernel which may yield effective gap to cut off the information flow.
3. It is interesting to consider both the probe and environment dynamics holographically without introducing the probe kinetic energy by hand.

II. Decoherence of Topological qubits

Facts about TI/TSC in our context

1) They are gapped systems and characterized by the robust gapless edge modes.
2) They can be understood as anomaly inflow. The transports of the edge modes are dictated by quantum anomaly. (c.f. Chiral Magnetic Effect)
3) The anomaly transport is known to be dissipationless, ie, there is no generation of entropy. (c.f. Battacharya et al, 02)
4) The robustness is implied by no-dissipation, but we may ask:

a. What is the form of the influence functional? Involves only fluctuation kernel?

b. Does no-dissipation imply also decoherence free?

Majorana modes

1) We consider the simplest topological edge modes, the Majorana modes, ie, $\gamma_a^\dagger = \gamma_a \ , \qquad \{\gamma_a, \gamma_b\} = 2\delta_{a,b}$
2) A topological qubit = 2 (separated) Majorana modes, ie,

$$d_i = (\gamma_{2i-1} + i\gamma_{2i})/2 \qquad \{d_i, d_i^\dagger\} = 1$$

3) Kitaev chain (1D p-wave TSC) can realize Majorana edge modes: (c.f. Kitaev, 03)

$$H_F = w\sum_{i=1}^{N-1}(d_i - d_{i+1}^\dagger)(d_{i+1} + d_{i+1}^\dagger) + 2v\sum_{i=1}^{N}(d_i^\dagger d_i - 1/2) \ , \qquad [(-1)^{\sum_i d_i^\dagger d_i}, H_F] = 0$$

$$H_F \sim v\sum_{i=1}^{N}\gamma_{2i-1}\gamma_{2i} + w\sum_{i=1}^{N-1}\gamma_{2i}\gamma_{2i+1}$$

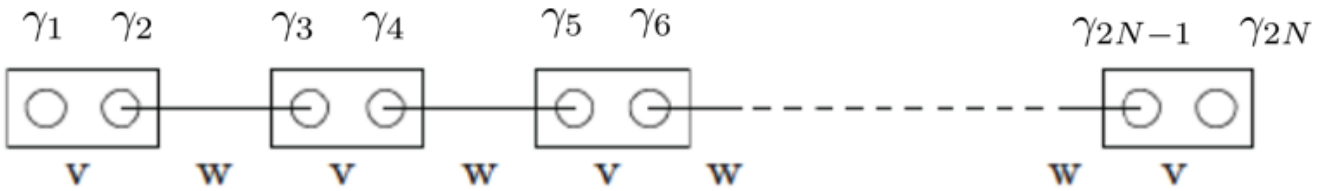

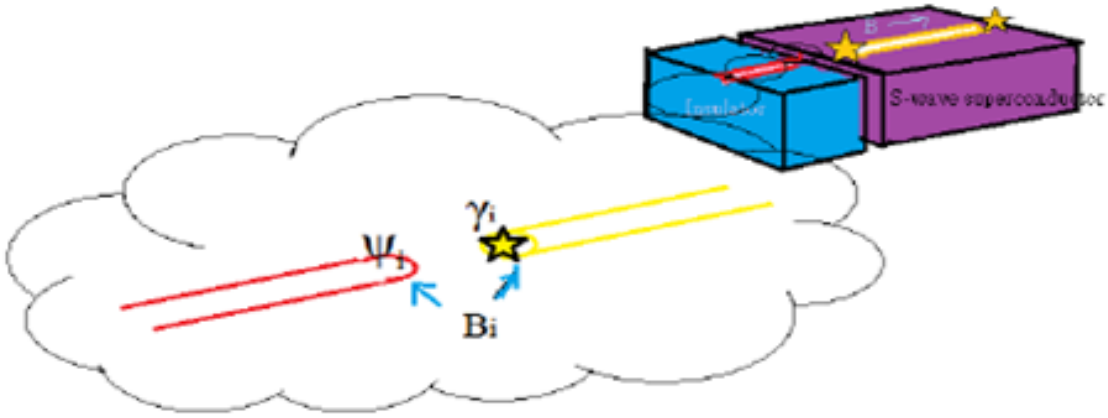
S-wave superconductor
γ_i
ψ_i
B_i

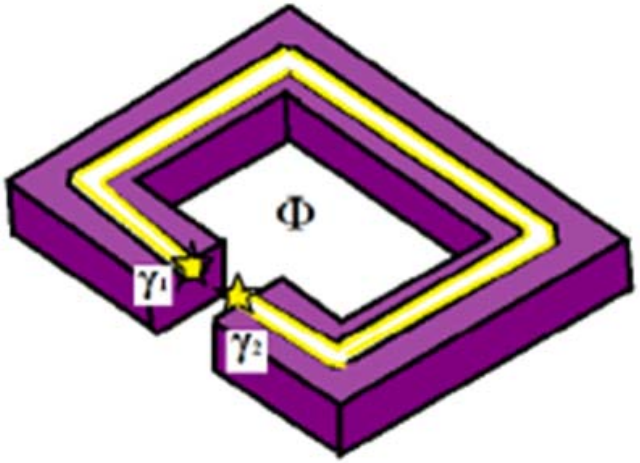
Φ
γ_1
γ_2

Topological qubits as open system

1) We put these Majorana edge modes in contact with the Luttinger/Fermi liquids, ie, with Ohmic type spectral density (for operator $\mathcal{O}_{a,ab}$ below)

$$S_{spec}^{(env)}(\omega) = c_0(Q)\omega^Q \, e^{-\omega^2/\Gamma_0^2} \,, \qquad Q \geq 0$$

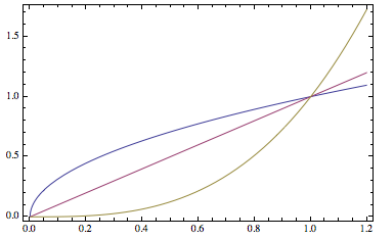

2) The total Hamiltonian is

$$H_{total} = H_{probe} + H_{env}^{(Ohmic)} + V$$

$$H_{probe} = 0 \,, \qquad V = \sum_a B_a \gamma_a \mathcal{O}_a + \sum_{a>b} B_{ab} \gamma_a \gamma_b \mathcal{O}_{ab}$$

3) Further assuming all terms in V commute with each other. Then, the reduced dynamics can be solved exactly in the interaction picture.

Reduced dynamics

1) The reduced dynamics is dictated by the ``influence functional", which only involves fluctuation kernel, ie,

$$\langle \tilde{\mathrm{T}} \cosh \mathbf{O}_M(t) \mathrm{T} \cosh \mathbf{O}_M(t) \rangle_{\mathcal{E}}$$
$$\approx \frac{1}{2}(e^{2B_M^2 \int^t d\tau \int^t d\tau' \overline{G}_{M,sym}(\tau-\tau')} + 1) ,$$
$$\langle \tilde{\mathrm{T}} \sinh \mathbf{O}_M(t) \mathrm{T} \sinh \mathbf{O}_M(t) \rangle_{\mathcal{E}}$$
$$\approx \frac{1}{2}(e^{2B_M^2 \int^t d\tau \int^t d\tau' \overline{G}_{M,sym}(\tau-\tau')} - 1) .$$

$$\langle \mathrm{T}_C \, \mathcal{O}_a(t) \gamma_a \gamma_a \mathcal{O}_a(t') \rangle_{\mathcal{E}}$$
$$= \langle \mathcal{O}_a(t) \mathcal{O}_b(t') \rangle_{\mathcal{E}} \Theta(t-t') + \langle \mathcal{O}_a(t') \mathcal{O}_a(t) \rangle_{\mathcal{E}} \Theta(t'-t)$$

2) There is no dissipation kernel appearing in the final form of the reduced dynamics. This is related to the fact that the Majorana modes are dissipationless, i.e., generating no heat.
3) The influence functional has qualitatively different behaviors for super- and sub-Ohmic fluctuation kernel.

Special features

1) The symmetric Green function appearing above is the Majorana-dressed one, ie, bosonic-like:

2) Turn out that this time factor for Ohmic-like spectrum has a closed form, and has a critical behavior at Q=1.

$$\langle \mathrm{T}_C\, \mathcal{O}_a(t)\gamma_a\gamma_a\mathcal{O}_a(t')\rangle_{\mathcal{E}} = \langle \mathcal{O}_a(t)\mathcal{O}_b(t')\rangle_{\mathcal{E}}\Theta(t-t') + \langle \mathcal{O}_a(t')\mathcal{O}_a(t)\rangle_{\mathcal{E}}\Theta(t'-t)$$

Time behavior of influence functional

$$\alpha(t) = e^{2B^2 \int^t d\tau \int^t d\tau' \overline{G}_{sym}(\tau-\tau')} = e^{-2B^2 |\alpha_{1,2}| I_Q(t;\mu=0,\Gamma_0)}$$

$(Q = 2\kappa - 1$ for fermionic and $Q = 2\Delta - 4$ for bosonic environment)

$Q \leq 1$ (Ohmic and sub-Ohmic)

$Q > 1$ (super Ohmic)

Non-Markovian, ie, information backflow

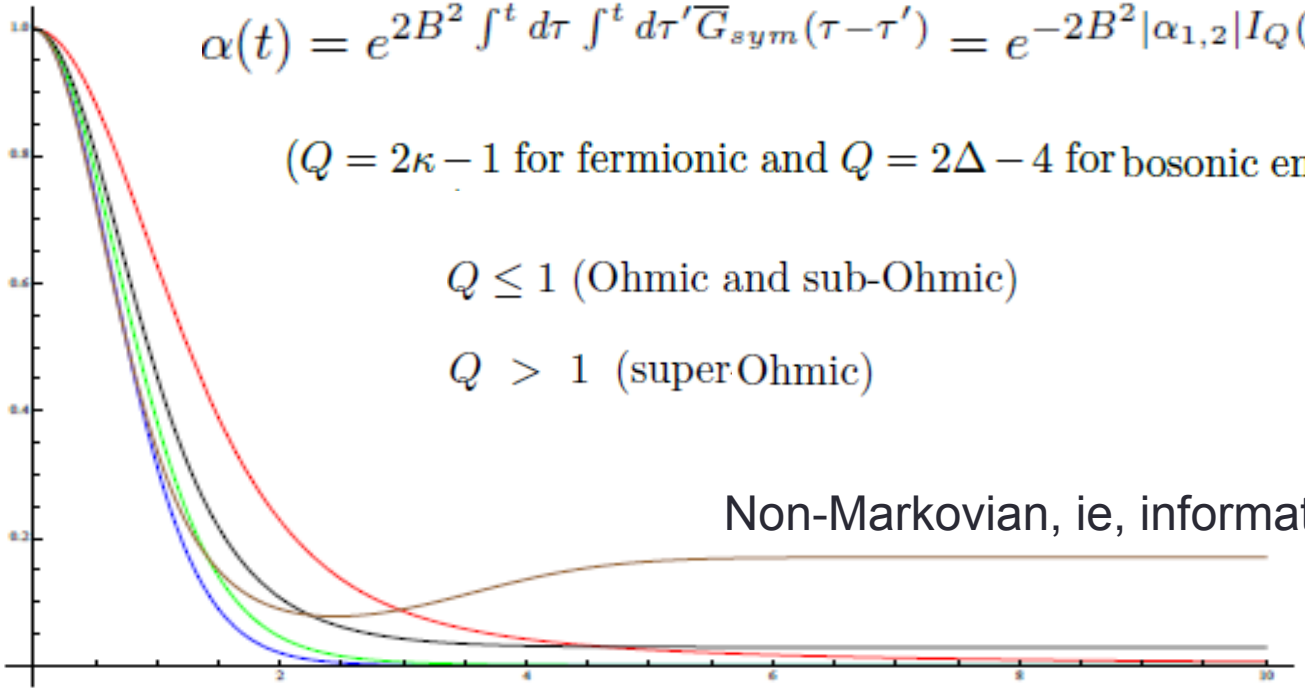

FIG. 3: $e^{-I_Q(t;\mu=0,\Gamma_0=1)}$ v.s. t for $Q = 0.5$(blue), 0.9(green), 1(red), 2 (black) and 4 (brown). This factor controls the time dependence of the influence functional. We can see that there is a critical value at $Q = 1$ beyond which this factor will have a pattern of drop-dip-flat and will not decay to zero.

Z2 parity

1) We prepare pure initial states in the qubit basis, ie,

$$d_i|1\rangle = |0\rangle\,, \qquad d_i = (\gamma_{2i-1} + i\gamma_{2i})/2\,, \qquad \gamma_a^\dagger = \gamma_a$$

2) Z2 parity: $i\gamma_1\gamma_2|0\rangle = |0\rangle\,, \qquad i\gamma_1\gamma_2|1\rangle = -|1\rangle$
3) The interactions with single Majorana mode break Z2.
4) Z2 parity turns out to relevant for decoherence pattern

Single topological qubit

1) Pure initial state: $\rho_{\mathcal{P}}(t=0) = \begin{pmatrix} a_{00} & a_{01} \\ a_{01} & a_{11} \end{pmatrix}$

$$\alpha(t) = e^{2B^2 \int^t d\tau \int^t d\tau' \overline{G}_{sym}(\tau-\tau')} = e^{-2B^2 |\alpha_{1,2}| I_Q(t;\mu=0,\Gamma_0)}$$

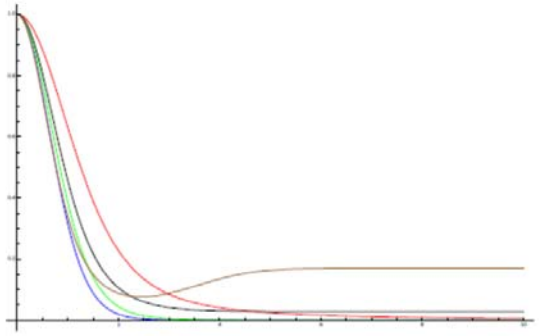

2) For Z2-preserving interactions:

$$\rho_r^b(t) = \begin{pmatrix} a_{00} & a_{01}\alpha(t) \\ a_{10}\alpha(t) & a_{11} \end{pmatrix}$$

3) For Z2-breaking interactions:

$$\rho_r^f(t) = \frac{1}{2} \begin{pmatrix} 1 + (2a_{00} - 1)\alpha^2(t) & 2a_{01}\alpha(t) \\ 2a_{10}\alpha(t) & 1 + (2a_{11} - 1)\alpha^2(t) \end{pmatrix}$$

4) The Z2 parity prevents from complete thermalization into Gibbs state.

Two T-qubits in Z2 environments

The red lines all turn into the pointer states but the blue lines do not.

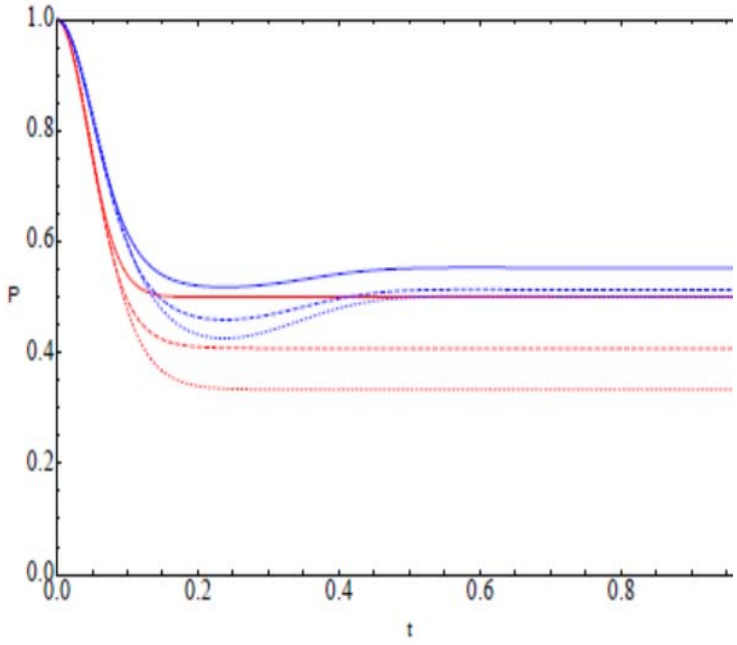

FIG. 6: Purity vs t for $\Delta = 2.3$ (red) and $\Delta = 4.1$ (blu initial states $|(e_1, e_2, e_3, e_4)\rangle = |(1,0,0,1)\rangle$ (solid), $|(2,$ (dashed), $|(1,1,0,1)\rangle$ (dotted).

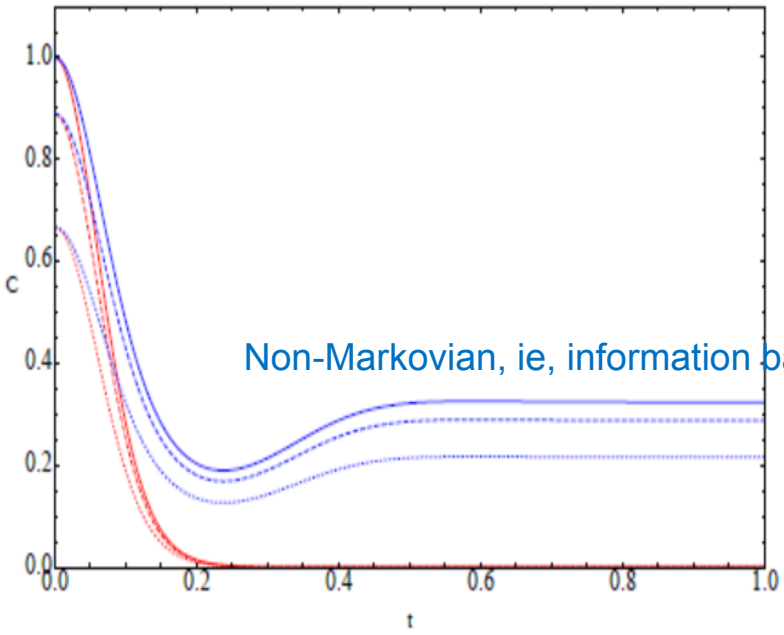

Non-Markovian, ie, information backflow

FIG. 7: Concurrence vs t for the states and environments specified in Fig. 6.

Two T-qubits in no-Z2 environments

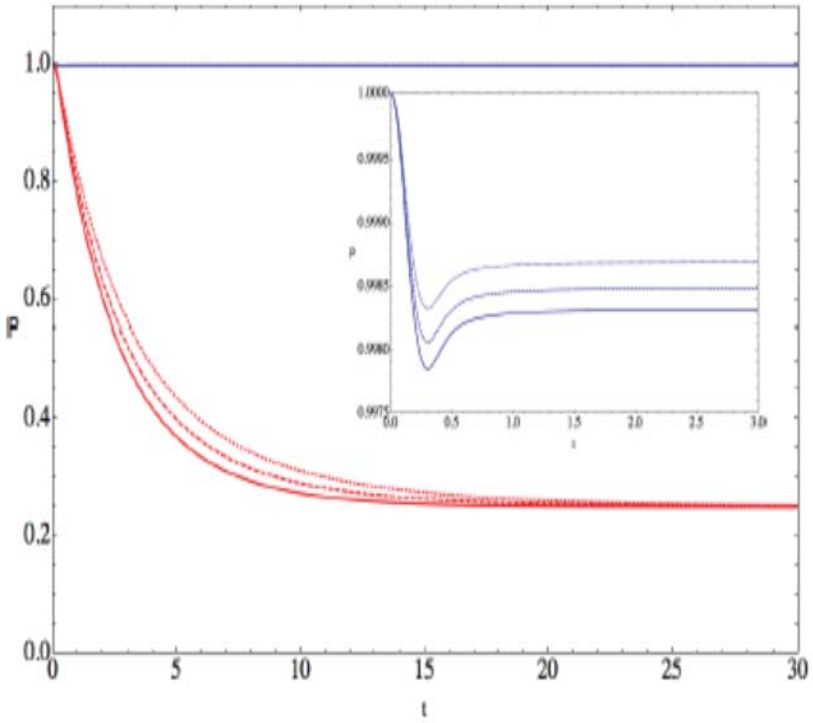

FIG. 4: Purity vs t for $\kappa = 0.5$ (red) and $\kappa = 2$ (blue) with initial states $|(e_1, e_2, e_3, e_4)\rangle = |(1, 0, 0, 1)\rangle$ (solid), $|(2, 1, 0, 2)\rangle$ (dashed), $|(1, 1, 0, 1)\rangle$ (dotted). The inset is to magnify the early time region of $\kappa = 2$ cases.

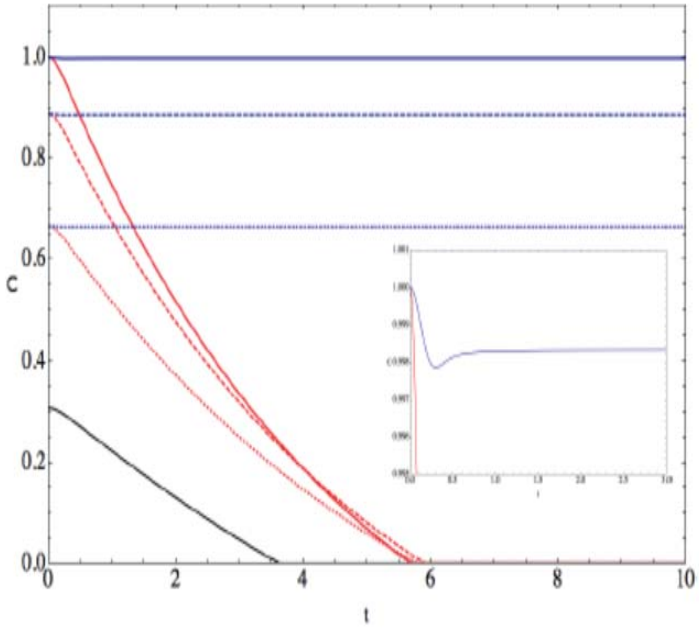

FIG. 5: Concurrence vs t for the states and environments specified in Fig. 4. The inset shows the solid lines enlarged at short time. Here we add a black solid line representing the concurrence pattern of the initial state $|(e_1, e_2, e_3, e_4)\rangle = |(2, 2, 1, 2)\rangle$ in the $\kappa = 0.5$ environment to show its concurrence does not diminish with the other red lines at the same time.

C.f. the non-topological qubits

All decohere completely even in the super-Ohmic environment.

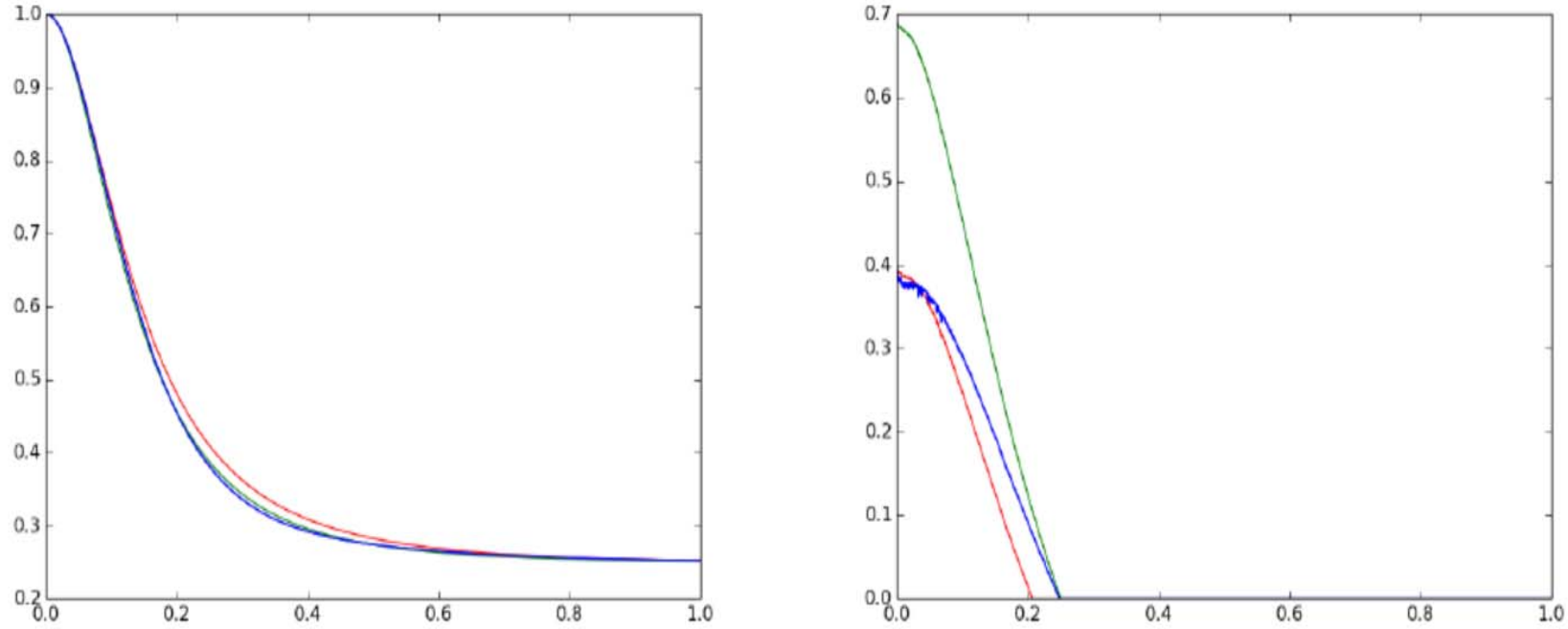

Figure 4: Super-Ohmic environment with $\mu = 0$ and $\kappa = 1.5$; the coupling constant g=0.1. the cut-off function is $\frac{100}{100+\omega^2}$ with $\Gamma_w = 10$. Red line for $(a^2, b^2, c^2, d^2) = (0.6, 0.0, 0.2, 0.2)$. Blue line for $(a^2, b^2, c^2, d^2) = (0.0, 0.6, 0.2, 0.2) = (0.2, 0.2, 0.6, 0.0)$. Green line for $(a^2, b^2, c^2, d^2) = (0.2, 0.0, 0.6, 0.2)$. Left: $Tr\rho^2$. Right : The concurrence.

C.f. Spin-Boson model

ref. S.T. Wu PRA89p034301

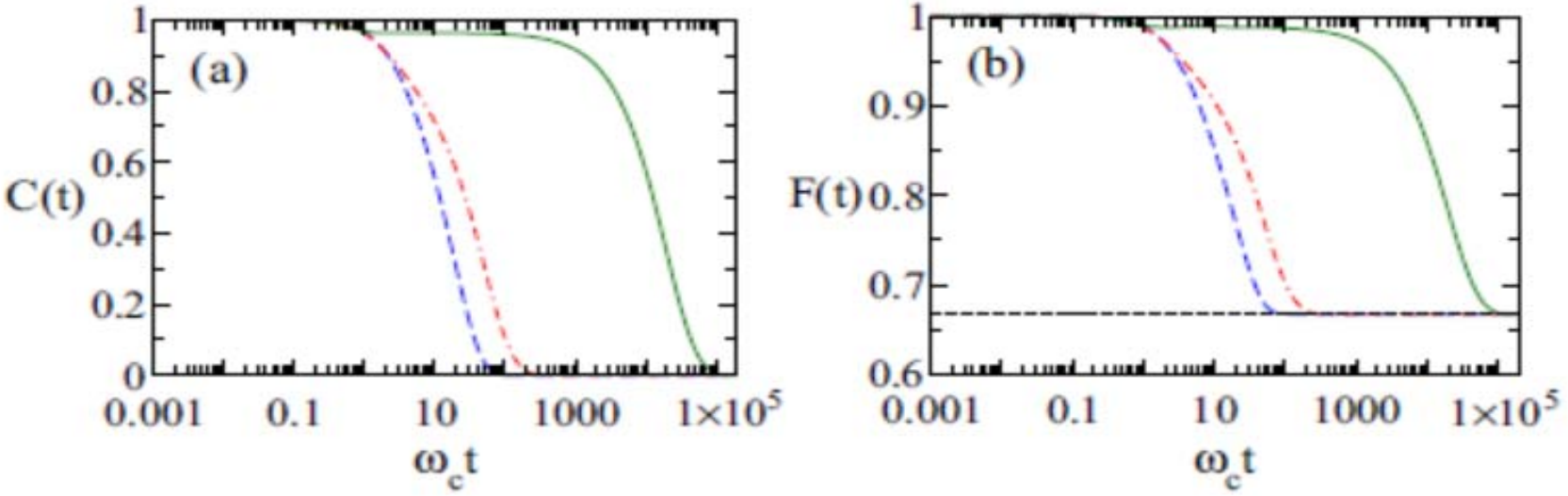

FIG. 3. (Color online) Time evolution for the (a) concurrence and (b) maximum teleportation fidelity for the Bell state (12) at weak environment coupling ($\eta_0 = 0.01$) when the spectral function is sub-Ohmic ($s = 1/2$, blue dashed curves), Ohmic ($s = 1$, red dot-dashed curves), and super-Ohmic ($s = 3$, green solid curves). The horizontal dashed line in (b) indicates the classical limit $F = \frac{2}{3}$.

Effective gap-ness

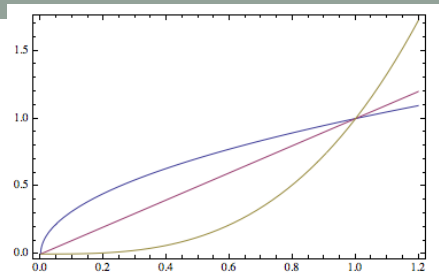

1) The quantum information of the probe is carried away by the collective excitations of the environment, which is specified by the spectral density.

2) The Ohmic-like spectrum has no gap at low energy, and one would expect the complete decoherence.

3) However, the super-Ohmic spectrum suppress more the low energy modes than the higher energy ones.

4) Adding the topological nature of the Majorana modes, we see an effective gap emerging for super-Ohmic cases.

Thanks.